SCIENTIFIC REPORTS

OPEN

Strong One-Dimensional Characteristics of Hole-Carriers in ReS$_2$ and ReSe$_2$

B. S. Kim[1,2,3], W. S. Kyung[1,2,4], J. D. Denlinger[4], C. Kim[1,2] & S. R. Park[3]

Each plane of layered ReS$_2$ and ReSe$_2$ materials has 1D chain structure, from which intriguing properties such as 1D character of the exciton states and linearly polarized photoluminescence originate. However, systematic studies on the 1D character of charge carriers have not been done yet. Here, we report on systematic and comparative studies on the energy-momentum dispersion relationships of layered transition metal dichalcogenides ReS$_2$ and ReSe$_2$ by angle resolved photoemission. We found that the valence band maximum or the minimum energy for holes is located at the high symmetric Z-point for both materials. However, the out-of-plane (k_z) dispersion for ReSe$_2$ (20 meV) is found to be much smaller than that of ReS$_2$ (150 meV). We observe that the effective mass of the hole carriers along the direction perpendicular to the chain is about 4 times larger than that along the chain direction for both ReS$_2$ and ReSe$_2$. Remarkably, the experimentally measured hole effective mass is about twice heavier than that from first principles calculation for ReS$_2$ although the in-plane anisotropy values from the experiment and calculations are comparable. These observation indicate that bulk ReS$_2$ and ReSe$_2$ are unique semiconducting transition metal dichalcogenides having strong one-dimensional characters.

Layered transition-metal dichalcogenides (TMDs) have been extensively studied in recent years because of their potential as electronic materials for future devices. Their intriguing characters of the electronic structures such as the valley degeneracy[1] and spin-valley-layer locking[2–4], provide added value for valley- and spintronic applications. While some of them even exhibit superconductivity and charge density waves originating from the electron-phonon and electron-electron interactions due to their low electronic dimensionality (e.g. in NbSe$_2$[5,6]), most of the studies have been focused on Mo and W compounds due to their semi-conducting properties and close to ideal 2 dimensionality[7–11].

Very recently, layered ReS$_2$ and ReSe$_2$ began to draw attention as their layer-layer interactions are much weaker than other layered TMDs[12]. More interestingly, ReS$_2$ and ReSe$_2$ have one-dimensional (1D) characters in their structure as well as optical and electrical properties due to the formation of Re chain structure stemming from the distortion in the 1T structural phase[12–14]. High-resolution transmission electron microscopy and electron diffraction studies reveal distorted 1T structure with Re chain formation[12]. Such structure distortion is directly related to the high anisotropy in the Raman response from in-plane lattice vibrations[14–19]. It also affects optical properties, e.g., anisotropic character in optical absorption or photoluminescence comes from that of excitons[20–24]. Electrical conductivity is also found to be much higher along the chain direction than the direction perpendicular to the chain[13,25,26].

As the above-mentioned intriguing 1D properties are determined by the characteristics of hole and electron band dispersions, electronic structure studies by angle resolved photoemission spectroscopy (ARPES) are naturally desired. Especially, the effective mass is a fundamental parameter that can be obtained from the energy and momentum dispersion relationship and governs the electrical and optical properties such as mobility, conductivity, light absorption and photoluminescence. In fact, a couple of ARPES studies on ReS$_2$ and ReSe$_2$ have been reported and the results indicate an in-plane anisotropy in the hole band dispersion as expected from the chain structures in ReS$_2$[27–29] and in ReSe$_2$[30]. However, obtaining very high-quality data needed to determine the effective mass for all directions turned out to be challenging. For example, the photon energy dependence of the

[1]Department of Physics and Astronomy, Seoul National University, Seoul, 08826, Korea. [2]Center for Correlated Electron Systems, Institute for Basic Science, Seoul, 08826, Korea. [3]Department of Physics, Incheon National University, Incheon, 22012, Korea. [4]Advanced Light Source, Lawrence Berkeley National Laboratory, Berkeley, CA, 94720, USA. Correspondence and requests for materials should be addressed to C.K. (email: changyoung@snu.ac.kr) or S.R.P. (email: AbePark@inu.ac.kr)
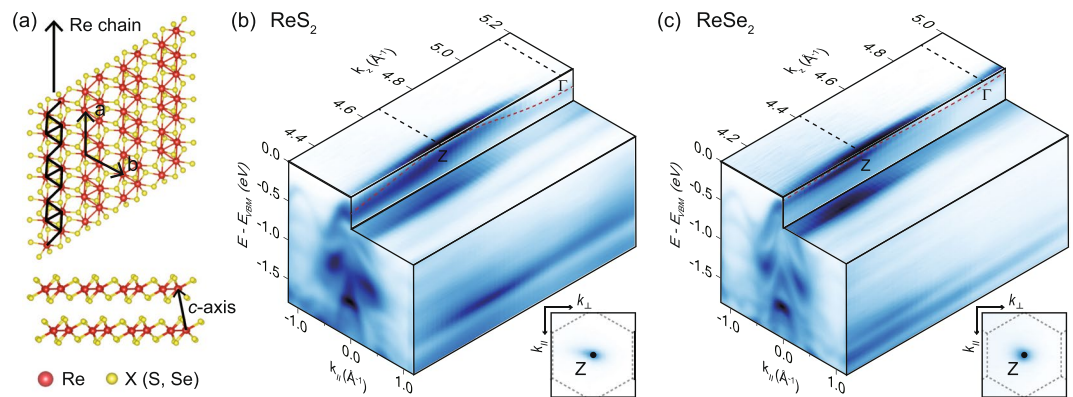
1

Figure 1. Crystal structure and out-of-plane valence band dispersions. (**a**) Top and side views of the crystal structure of ReX$_2$ (X = S, Se). It shows distorted 1 T structure with Re chains indicated by black solid lines. (**b,c**) Intensity plots of ReS$_2$ and ReSe$_2$ ARPES data in the energy and momentum space, respectively. k_Z dependent intensities are taken by using different photon energies from 60 eV to 110 eV with 2 eV step. k_Z is obtained with inner potentials of 17.8 and 12.4 eV for ReS$_2$ and ReSe$_2$, respectively. $k_{\parallel}$ and $k_{\perp}$ are in-plane momentum parallel and perpendicular to the chain, respectively. Red dashed lines are guides to eye for k_z dispersion of the top-most valence bands. Insets are 2D constant energy (E = E$_{VBM}$) intensity map in the momentum-space (as functions of $k_{\parallel}$ and $k_{\perp}$) at the k_z = Z-point. Note that there is a single peak at the zero in-plane momentum point (Z-point).

valence band dispersion for ReS$_2$ appears to be very different among the reported results[27,29]. In addition, direct comparison between measured valence band dispersions of ReS$_2$ and ReSe$_2$, for which lattice parameters are quite different[31], are difficult because the data were taken in different Brillouin zones for ReS$_2$ and ReSe$_2$[29,30].

In order to resolve aforementioned issues, we have performed systematic ARPES studies on ReS$_2$ and ReSe$_2$. Our goal is to take data for the entire momentum space which is good enough to do quantitative analysis and obtain in-plane anisotropy in the effective hole mass for the two materials for a comparative study. Our data show a striking difference from what were reported in previous experimental and theoretical studies[29,30,32]. (1) The valence band maximum (VBM) is located at the Z-point for both systems, while it was reported in a previous ARPES study reported that VBM of ReSe$_2$ may be located at non-high-symmetric momentum point[30,33]. (2) The k_z dispersion of ReSe$_2$ is much smaller than that of published quasiparticle band structure within the LDA + GdW approximation[32]. (3) The effective hole masses along and perpendicular to the chain direction are quite different from the reported experimental and theoretical values[29,30,34].

Results and Discussion

Valence band maximum of ReSe$_2$ and ReS$_2$.

ReS$_2$ and ReSe$_2$ are layered materials in which the van der Waals interaction between layers is extremely weak, even weaker than other TMDs[12]. The crystal structure for both ReS$_2$ and ReSe$_2$ is the so-called distorted 1T structure. Re atoms show a hexagonal network but the structure is distorted to have chain structures as indicated by black lines in Fig. 1(a). The 1D chain structure makes these materials unique among TMDs in that optical and electrical properties carry 1D characteristics[14–26].

The inner potential can be estimated from the k_z dispersion of electronic band (Fig. 1(b) and (c)) with the reciprocal lattice vector c^*. Based on the results of reported X-ray diffraction measurements[31], the reciprocal lattice vector c^* is calculated to be 1.032 Å^{-1} (0.984 Å^{-1}) for ReS$_2$ (ReSe$_2$). The inner potential is estimated to be V_0 = 17.8 and 12.4 eV for ReS$_2$ and ReSe$_2$. These estimated values are similar to those of other TMDs[35,36].

ARPES experiments are performed on ReS$_2$ and ReSe$_2$ to obtain the energy-and-momentum dispersion of the hole carriers. ARPES intensities as a function of the energy referenced to the valence band maximum (E$_{VBM}$) are mapped along two momentum directions, parallel to chain ($k_{\parallel}$) and perpendicular to the layer (k_z) (Fig. 1(b,c)). While several band dispersions are observed within the energy range, the top-most valence band is of interest as it determines the low energy properties of the materials such as electrical conductivity. Due to the layered structure, the top-most bands of ReS$_2$ and ReSe$_2$ show relatively weak dispersions along k_z than along in-plane momentum. Interestingly, we observed as shown in Fig. 1 that the k_z dispersion of ReSe$_2$ (about 20 meV) is even weaker compared to that of ReS$_2$ (about 150 meV) which is known as a material with very weak inter-layer interaction[12]. Therefore, our results show an evidence for even smaller interaction between layers in ReSe$_2$.

Our photon energy dependence data reveal that VBM is located at Z for both ReS$_2$ and ReSe$_2$ as indicated by the red dashed lines in Fig. 1(b,c). While previous ARPES studies also showed that VBM of ReS$_2$ is located at Z, VBM of ReSe$_2$ has been under debate. Hart et al. reported that the k_z for VBM of ReSe$_2$ is the same as the Z-point but the in-plane momentum was reported to be non-zero[30]. More recently, Eickholt et al. reported two VBM of ReSe$_2$[33]. One of them is at Z and the other is away from Z. But their experiment could not decide which is global VBM, since data quality is not good enough. The global VBM of ReSe$_2$ can be decided to be located at Z due to high quality data. Please refer to the supplementary materials for more details. In fact, we find that ReSe$_2$ result about VBM is consistent with a recent theoretical prediction as well[32].
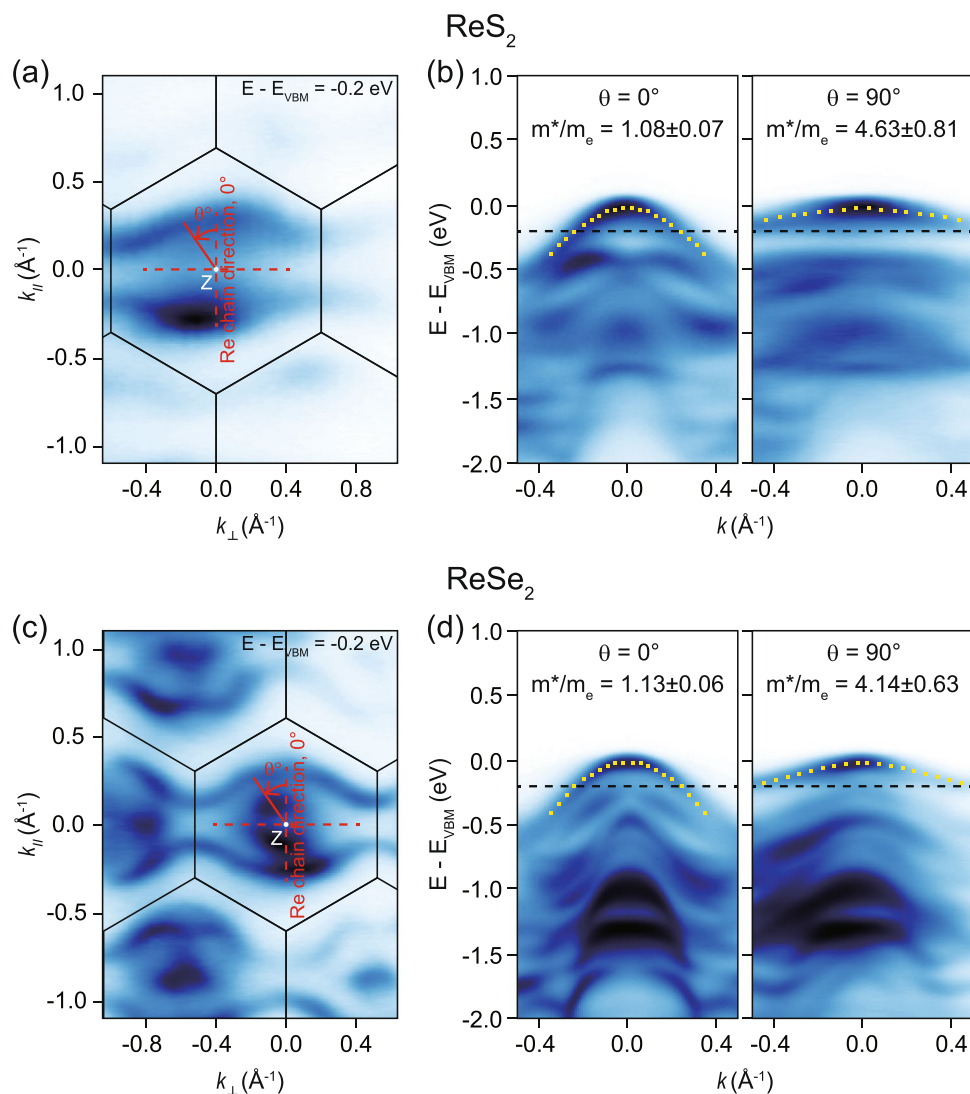
ReS$_2$

ReSe$_2$

Figure 2. In-plane valence band dispersions near the valence band maximum. Constant energy (E-E$_{VBM}$ = − 0.2 eV) ARPES maps of ReS$_2$ (**a**) and ReSe$_2$ (**c**). The photon energy used for the experiment was 70 eV for ReS$_2$ and 68 eV for ReSe$_2$. For these photon energies, k_z = Z point (white dot) where VBM is located is included in the data. Red solid and dashed lines in (**a,c**) indicate the direction parallel and perpendicular to the Re chain direction, respectively. θ is defined as the relative angle from the direction along the chain as shown in the figure. The honey comb structured line indicates the projected Brillouin zone boundary. (**b,d**) High symmetric cuts along (θ = 0°) and perpendicular (θ = 90°) to the Re chain. The dotted lines in (**b,d**) are quadratic fit to the top-most bands. The effective masses of hole carriers of ReX$_2$ extracted from the fitting functions are shown in the figures.

Directional dependence of effective hole masses in ReS$_2$ and ReSe$_2$.   In order to investigate the effective mass of the hole carrier, we analyze ARPES data obtained in the in-plane momentum space that includes the Z-point. As shown in Fig. 2(a,c), constant energy maps of ARPES intensities of ReS$_2$ and ReSe$_2$ at E-E$_{VBM}$ = − 0.2 eV show two-fold symmetry and strong anisotropic band contours which are not closed along the direction perpendicular to the chain. These observations indicate much smaller band dispersion along the direction perpendicular to the chain. The top-most band dispersions, which we are interested in, along the chain are much stronger than those along the other for both ReS$_2$ and ReSe$_2$. For quantitative analysis, we try to fit the band dispersions with a quadratic function for which the effective mass is a free parameter[32]. The dotted lines in Fig. 2(b,d) indicate the fit functions. So, obtained effective masses along the direction perpendicular to the chain (4.63 m$_e$ for ReS$_2$ and 4.14 m$_e$ for ReSe$_2$) are much heavier than the effective masses along chain (1.08 m$_e$ for ReS$_2$ and 1.13 m$_e$ for ReSe$_2$). That is, the effective mass along the chain is about 4 times lighter than that perpendicular to the chain for both ReS$_2$ and ReSe$_2$. This in-plane anisotropy value in the effective hole mass is the largest among semiconducting TMDs[37,38].

The valence band dispersion can also be analyzed for different theta angle and corresponding effective hole mass can be obtained. Shown in Fig. 3(a,b) are ARPES data along in-plane momentum set by the θ angle defined in Fig. 2(a). The data are subsequently analyzed and the corresponding effective hole mass is obtained for a
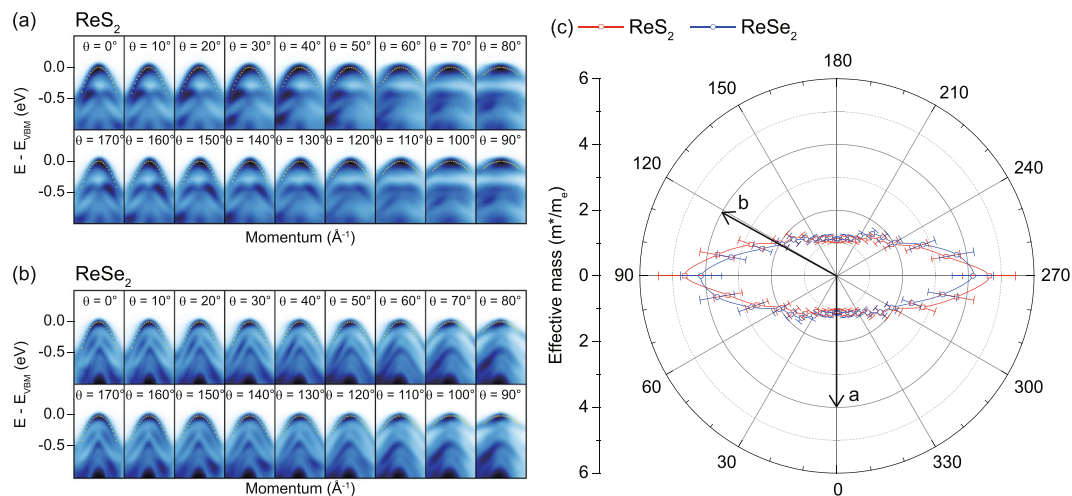
Figure 3. Anisotropic effective hole masses. ARPES cut data along the in-plane momentum defined by the angle θ (see Fig. 2(a) for definition) for (**a**) ReS$_2$ and (**b**) ReSe$_2$. All the data sets are centered around the Z-point at which VBM is located. The dotted lines indicate a quadratic function fitting the dispersions of the top-most bands. The effective mass from the quadratic fit function for each angle can be extracted and is plotted for ReS$_2$ and ReSe$_2$ in (**c**). Arrows indicate crystallographic orientation of ReX$_2$.

systematic study of direction dependence. We notice the top-most band can be fitted well with a quadratic function indicated by dotted lines, which makes us confident in our analysis. The extracted effective mass from the quadratic function is plotted in polar coordinate as a function of the theta angle in Fig. 3(c). The plot clearly shows two-fold symmetry and strong in-plane anisotropy of the effective hole mass for both ReS$_2$ (red) and ReSe$_2$ (blue). There is an important point to discuss in comparison with the results of first principles calculations on ReS$_2$. The experimentally observed effective mass is about twice larger than that from the first principles calculations. The effective mass from the first principles calculations is 2.4 m$_e$ along the direction perpendicular to the chain and 0.8 m$_e$ along the chain[27]. The electron-electron and electron-phonon interactions or atomic spin-orbit coupling of Re atom which were not considered in the calculation may play a crucial role in the clear enhancement of the effective hole mass.

Conclusions

In this study, we performed systematic ARPES studies of ReS$_2$ and ReSe$_2$ to reveal the energy-momentum dispersion relationships of the top most valence bands. We found that ReSe$_2$ have much smaller k_z dispersion than ReS$_2$, indicating the more 2D-like feature in ReSe$_2$ than in ReS$_2$. We systematically investigated in-plane directional dependence of the effective hole masses of ReSe$_2$ and ReSe$_2$. The effective masses show strong anisotropy, about 4 times lighter along the chain than the direction perpendicular to the chain. In-plane anisotropy of the hole effective masses in ReS$_2$ and ReSe$_2$ is larger than that in black phosphorus which also shows anisotropic electrical and optical properties[39,40]. Therefore, ReS$_2$ and ReSe$_2$ are quasi 1D materials in terms of the low energy hole carrier dynamics, which makes ReS$_2$ and ReSe$_2$ promising bulk materials for 1D semiconducting electronics. The effective mass of ReS$_2$ observed by ARPES is found to be significantly enhanced compared to that from first principles calculations. Electron-electron and electron-phonon interactions or atomic spin-orbit coupling of Re atom may be attributed to the mass enhancement[41]. The quasi 1D character of the hole carriers as well as possibility of the electron-electron and electron-phonon interactions may lead to charge density wave order if enough amount of hole carriers are doped into ReS$_2$ and ReSe$_2$[42].

Methods

ARPES measurement. We performed ARPES experiments at the beamline 4.0.3.2 (MERLIN) of the Advanced Light Source at the Lawrence Berkeley National Laboratory equipped with VG-Scienta R8000 electron analyzer. All samples are cleaved *in-situ* and data were taken at 200 K to avoid the charging effect in a vacuum better than 6×10^{-11} Torr. with linearly polarized light. For the k$_z$ dependence experiment, photon energies between 60 and 110 eV with 2 eV energy step were used. The total energy resolution was better than 20 meV with a momentum resolution of 0.004 Å^{-1}.

References

1. Xiao, D., Liu, G.-B., Feng, W. X., Xu, X. & Yao, W. Coupled Spin and Valley Physics in Monolayers of MoS2 and Other Group-VI Dichalcogenides. *Phys. Rev. Lett.* **108**, 196802 (2012).
2. Xu, X., Yao, W., Xiao, D. & Heinz, T. F. Spin and pseudospins in layered transition metal dichalcogenides. *Nat. Phys.* **10**, 343–350 (2014).
3. Jones, A. M. *et al.* Spin-layer locking effects in optical orientation of exciton spin in bilayer WSe$_2$. *Nat. Phys.* **10**, 130–134 (2014).
4. Yao, W. *et al.* Direct observation of spin-layer locking by local Rashba effect in monolayer semiconducting PtSe$_2$ film. *Nat. Commun.* **8**, 14216 (2017).
5. Frindt, R. F. Superconductivity in Ultrathin NbSe$_2$ Layers. *Phys. Rev. Lett.* **28**, 299 (1972).
6. Arguello, C. J. *et al.* Visualizing the charge density wave transition in 2H-NbSe$_2$ in real space. *Phys. Rev. B* **89**, 235115 (2014).

7. Jin, C. H. *et al*. Ultrafast dynamics in van der Waals heterostructures. *Nat. Nanotech.* **13**, 994–1003 (2018).
8. Rivera, P. *et al*. Interlayer valley excitons in heterobilayers of transition metal dichalcogenides. *Nat. Nanotech.* **13**, 1004–1015 (2018).
9. Manzeli, S., Ovchinnikov, D., Pasquier, D., Yazyev, O. V. & Kis, A. 2D transition metal dichalcogenides. *Nat. Rev. Mater.* **2**, 17033 (2017).
10. Wang, G. *et al*. *Colloquium*: Excitons in atomically thin transition metal dichalcogenides. *Rev. Mod. Phys.* **90**, 021001 (2018).
11. Chhowalla, M. *et al*. The chemistry of two-dimensional layered transition metal dichalcogenide nanosheets. *Nat. Chem.* **5**, 263–275 (2013).
12. Tongay, S. *et al*. Monolayer behavior in bulk ReS_2 due to electronic and vibrational decoupling. *Nat. Commun.* **5**, 3252 (2014).
13. Tiong, K. K., Ho, C. H. & Huang, Y. S. The electrical transport properties of ReS_2 and $ReSe_2$ layered crystals. *Solid State Commun.* **111**, 635–640 (1999).
14. Wolverson, D., Crampin, S., Kazemi, A. S., Ilie, A. & Bending, S. J. Raman Spectra of Monolayer, Few-layer, and bulk $ReSe_2$: An Anistropic Layered Semiconductor. *ACS Nano* **8**, 11154–11164 (2014).
15. Lorchat, E., Froehlicher, G. & Berciaud, S. Splitting of Interlayer Shear Modes and Photon Energy Dependent Anisotropic Raman Response in *N*-Layer $ReSe_2$ and ReS_2. *ACS Nano* **10**, 2752–2760 (2016).
16. Chenet, D. *et al*. In-Plane Anisotropy in Mono- and Few-Layer ReS_2 Probed by Raman Spectroscopy and Scanning Transmission Electron Microscopy. *Nano Lett.* **15**, 5667–5672 (2016).
17. He, R. *et al*. Coupling and Stacking Order of ReS_2 Atomic Layers Revealed by Ultralow-Frequency Raman Spectroscopy. *Nano Lett.* **16**, 1404–1409 (2016).
18. Nagler, P., Plenchinger, G., Schüller, C. & Korn, T. Observation of anisotropic interlayer Raman modes in few-layer ReS_2. *Phys. Status Solidi RRL* **10**, 185–189 (2016).
19. Li, L. *et al*. Strong In-Plane Anisotropies of Optical and Electrical Response in Layered Dimetal Chalcogenide. *ACS Nano* **11**, 10264–10272 (2017).
20. Ho, C. H., Huang, Y. S., Tiong, K. K. & Liao, P. C. Absorption-edge anisotropy in ReS_2 and $ReSe_2$ layered semiconductors. *Phys. Rev. B* **58**, 16130 (1998).
21. Zhong, H.-X., Gao, S. Y., Shi, J.-J. & Yang, L. Quasiparticle band gaps, excitonic effects, and anisotropic optical properties of the monolayer distorted 1T diamond-chain structures ReS_2 and $ReSe_2$. *Phys. Rev. B* **92**, 115438 (2015).
22. Aslan, O. B., Chenet, D. A., van der Zande, A. M., Hone, J. C. & Heinz, T. F. Linearly Polarized Excitons in Single- and Few-Layer ReS_2 Crystals. *ACS Photonics* **3**, 96–101 (2016).
23. Sim, S. *et al*. Selectively tunable optical Stark effect of anisotropic excitons in atomically thin ReS_2. *Nat. Commun.* **7**, 13569 (2016).
24. Sim, S. *et al*. Ultrafast quantum beats of anisotropic excitons in atomically thin ReS_2. *Nat. Commun.* **9**, 351 (2018).
25. Ho, C. H., Huang, Y. S. & Tiong, K. K. In-plane anisotropy of the optical and electrical properties of ReS2 and ReSe2 layered crystals. *J. Alloys Comp.* **317**, 222–226 (2001).
26. Hu, S. Y., Liang, C. H., Tiong, K. K., Huang, Y. S. & Lee, Y. C. Electrical Anisotropy of W-Doped $ReSe_2$ Crystals. *J. Electrochem. Soc.* **153**, J100–J102 (2006).
27. Biswas, D. *et al*. Narrow-band anisotropic electronic structure of ReS_2. *Phys. Rev. B* **96**, 085205 (2017).
28. Gehlmann, M. *et al*. Direct Observation of the Band Gap Transition in Atomically Thin ReS_2. *Nano Lett.* **17**, 5187–5192 (2017).
29. Webb, J. L. *et al*. Electronic band structure of ReS_2 by high-resolution angle-resolved photoemission spectroscopy. *Phys. Rev. B* **96**, 115205 (2017).
30. Hart, L. S. *et al*. Electronic bandstructure and van der Waals coupling of $ReSe_2$ revealed by high-resolution angle-resolved photoemission spectroscopy. *Sci. Rep.* **7**, 5145 (2017).
31. Ho, C. H., Huang, Y. S., Liao, P. C. & Tiong, K. K. Crystal structure and band-edge transition of $ReS_{1-x}Se_x$ layered compounds. *J. Phys. Chem. Solids* **60**, 1797–1804 (1999).
32. Arora, A. *et al*. Highly Anisotropic in-Plane Excitons in Atomically Thin and Bulklike 1T′-$ReSe_2$. *Nano Lett.* **17**, 3202–3207 (2017).
33. Eickholt, P. *et al*. Location of the valence band maximum in the band structure of anisotropic 1T′-$ReSe_2$. *Phys. Rev. B* **97**, 165130 (2018).
34. Yu, S. *et al*. Strain-engineering the anisotropic electrical conductance in ReS_2 monolayer. *Appl. Phys. Lett.* **108**, 191901 (2016).
35. Kim, B. S., Rhim, J.-W., Kim, B. Y., Kim, C. & Park, S. R. Determination of the band parameters of bulk 2H-MX_2 (M = Mo, W; X = S, Se) by angle-resolved photoemission spectroscopy. *Sci. Rep.* **6**, 36389 (2016).
36. Bovet, M. *et al*. Interplane coupling in the quasi-two-dimensional 1T-TaS_2. *Phys. Rev. B* **67**, 125105 (2003).
37. Miró, P., Audiffred, M. & Heine, T. An atlas of two-dimensional materials. *Chem. Soc. Rev.* **43**, 6537–6554 (2014).
38. Zibouche, N., Philipsen, P., Kuc, A. & Heine, T. Transition-metal dichalcogenide bilayers: Switching materials for spintronic and valleytronic applications. *Phys. Rev. B* **90**, 125440 (2014).
39. Xia, F., Wang, H. & Jia, Y. Rediscovering black phosphorus as an anisotropic layered material for optoelectronic and electronics. *Nat. Commun.* **5**, 4458 (2014).
40. Akahama, Y., Endo, S. & Narita, S.-I. Electrical Properties of Black Phosphorus Single Crystals. *J. Phys. Soc. Jpn.* **52**, 2148–2155 (1983).
41. Mahan, G. D. *Many-Particle Physics* (New York 1990).
42. Grüner, G. *Density Waves in Solids* (New York 1994).

Acknowledgements

Author Contributions

B.S.K. and W.S.K. performed ARPES measurements with the support from J.D.D.; B.S.K. analyzed the ARPES data; B.S.K., C.K. and S.R.P. wrote the paper; C.K. and S.R.P. are responsible for project direction and planning.

Additional Information

Supplementary information accompanies this paper at https://doi.org/10.1038/s41598-019-39540-4.

Competing Interests: The authors declare no competing interests.

Publisher's note: Springer Nature remains neutral with regard to jurisdictional claims in published maps and institutional affiliations.